Biochemical Pharmacology, Vol. 55, pp. 831–839, 1998.

ISSN 0006-2952/98/$19.00 + 0.00
PII S0006-2952(97)00561-3

Inhibition of CYP1A1-Dependent Activity by the Polynuclear Aromatic Hydrocarbon (PAH) Fluoranthene

Kristine L. Willett, Kurt Randerath,† Guo-Dong Zhou† and Stephen H. Safe*†*

*Department of Veterinary Physiology and Pharmacology, Texas A&M University, College Station, TX 77843-4466; and †Division of Toxicology, Baylor College of Medicine, Texas Medical Center, Houston, TX 77030, U.S.A.

ABSTRACT. Polynuclear aromatic hydrocarbons (PAHs) are ubiquitous environmental contaminants, and recently bioassay-based induction studies have been used to determine exposures to complex mixtures of PAHs. Induction of CYP1A1-dependent activity in H4IIE rat hepatoma cells has been used extensively as a bioassay for halogenated aromatic hydrocarbons and more recently for PAHs. Fluoranthene (FL) is a prevalent PAH contaminant in diverse environmental samples, and FL did not induce CYP1A1-dependent ethoxyresorufin *O*-deethylase (EROD) activity significantly in H4IIE cells. However, in cells cotreated with 2×10^{-5} M FL plus the potent inducers 2,3,7,8-tetrachlorodibenzo-*p*-dioxin (TCDD) or benzo[*k*]fluoranthene (BkF) (2×10^{-8} M), there was a significant decrease in EROD activities. Furthermore, treatment of TCDD-induced rat microsomes with FL caused an 80% decrease in EROD activity. Studies showed that FL did not affect induction of CYP1A1 protein or mRNA levels in H4IIE cells, and analysis of enzyme inhibition data using microsomal CYP1A1 indicated that FL noncompetitively inhibited CYP1A1-dependent activity. ^{32}P-Postlabeling revealed no significant FL–DNA adduct formation in H4IIE cells treated with FL. However, in cells cotreated with FL plus BkF or benzo[*a*]pyrene (BaP), certain PAH–DNA adducts were induced 2-fold. This study demonstrated that FL is an inhibitor of CYP1A1-dependent enzyme activity in rat hepatoma H4IIE cells and that the genotoxic potency of some carcinogenic PAHs may be modulated by FL in mixtures containing relatively high levels of this compound. BIOCHEM PHARMACOL **55**;6:831–839, 1998. © 1998 Elsevier Science Inc.

KEY WORDS. PAHs; fluoranthene; DNA adducts; H4IIE cells; CYP1A1; Ah receptor

PAHs§ are byproducts of incomplete combustion; they have been characterized extensively as atmospheric and aquatic contaminants, and they have been identified as major components in multiple chemical wastes [1–5]. The higher molecular weight PAHs have been linked to tumor formation and cancer in humans [6, 7], laboratory mammals [1], and fish [8]. FL, a component of various PAH mixtures, contains only four fused rings, and most studies indicate that FL exhibits relatively low carcinogenic activity. However, FL has been associated with immunotoxicity [9] including apoptotic murine T-cell death and growth arrest that were independent of the aryl hydrocarbon (Ah) receptor. FL potentiates the carcinogenicity of BaP in mouse skin [10], and lung tumors were found to develop in CD-1 mice treated with FL 1, 8, and 15 days after birth [11]. The *anti*-10b-N^2-deoxyguanosin-1,2,3-trihydroxy-1,2,3,10b-tetrahydrofluoranthene (*anti*-FADE) adduct was positively correlated with persistence and organ specificity for tumor formation [12].

Because of the toxicity and wide distribution of PAHs, bioassays are being developed to monitor PAHs in environmental samples [13, 14]. The H4IIE rat hepatoma cell bioassay, where CYP1A1-mediated induction of EROD activity is quantitated, has been used extensively to characterize the induction potency of various HAHs such as polychlorinated biphenyls (PCBs), polychlorinated dibenzo-*p*-dioxins, and dibenzofurans [15–18]. Because some PAHs, like HAHs, bind to the Ah receptor and induce EROD activity [19], our laboratory has investigated the potency of a series of PAHs in this H4IIE cell system [13]. BkF was the most potent inducer of EROD activity with relative potency or induction EFs compared with TCDD of 0.005 or 0.04, depending on the assay protocol [20]. In contrast, most of the lower molecular weight PAHs such as FL, phenanthrene, fluorene, acenaphthene, and naphthalene exhibit minimal induction activity [19 and unpublished results]. The following equation has been used for determining EQs for environmental samples containing mixtures of HAHs and PAHs where individual EFs are multiplied by their concentration in the sample: $EQ_{extract} = \Sigma([PAH]_1 EF_1 + \ldots + [PAH]_n EF_n)$. Additivity of the

‡ Corresponding author: Tel. (409) 845-5988; FAX (409) 862-4929.

§ *Abbreviations:* PAHs, polynuclear aromatic hydrocarbons; FL, fluoranthene; BkF, benzo[*k*]fluoranthene; BaP, benzo[*a*]pyrene; TCDD, 2,3,7,8-tetrachlorodibenzo-*p*-dioxin; EROD, ethoxyresorufin O-deethylase; EF, equivalency factor; HAHs, halogenated aromatic hydrocarbons; RAL, relative adduct labeling; and EQ, induction equivalents.

Received 28 April 1997; accepted 10 September 1997.

induction response is essential for utilizing this model. While the EQ approach has been largely accepted for hazard assessment of HAHs [15–18], there are some congeners in HAH mixtures that do not act additively. For example, when PLHC-1 fish liver cells were treated with 3,3′,4,4′-tetrachlorobiphenyl (PCB 77), EROD activity was reduced at higher concentrations (1 and 10 μM) compared with activity observed using 0.1 μM PCB 77. In the same study, immunoreactive CYP1A protein continued to increase at the higher concentrations of PCB 77 despite the decrease in enzyme activity [21].

FL is a poor inducer of EROD activity, and this is consistent with its low affinity for the AhR receptor. Because FL has been detected at high concentrations in diverse environmental samples [22–24], the possible nonadditive interactions of FL with PAHs, which are potent inducers of CYP1A1, were investigated, using the H4IIE rat hepatoma cell bioassay. FL significantly inhibited induction of EROD activity by BkF or TCDD in H4IIE cells, and, therefore, the mechanism of this inactivation process was investigated further. The results suggest that FL is a noncompetitive inhibitor of CYP1A1. Previous studies have identified other inhibitors of CYP1A1 activity, and these include tributyltin [25], aminoanthracene [26], substituted flavones [27], 2-phenylphenanthridinone [28], dihydrosafrole [29], and α-naphthoflavone [30–32]. To our knowledge, this is the first report of an environmentally significant PAH that inhibits the CYP1A1-dependent activity induced by another PAH. Antagonism by FL may be important in bioassays of PAH mixtures using CYP1A1-mediated endpoints. PAH–DNA adduct formation has been correlated with tumor formation in several different species [33–36]. BaP–DNA adducts are the most well characterized, and alkylation of the N-2 position on deoxyguanosine by the (+)-anti-BaP-7,8-diol-9,10 epoxide may be important for BaP-induced genotoxicity. The interaction of FL on adduct formation in H4IIE cells cotreated with BaP and BkF was also investigated. In our system, FL alone did not result in any adduct formation; however, the formation of specific BaP and BkF adducts was increased approximately 2-fold by cotreatment with FL.

MATERIALS AND METHODS

Cell Culture and EROD Assay

Rat hepatoma H4IIE cells were grown as a continuous cell line in α-minimum essential medium (α-MEM; Sigma) supplemented with 2.2 g/L sodium bicarbonate, 10% fetal bovine serum, and 10 mL/L antibiotic/antimycotic solution. Stock culture cells were grown in 150 cm^2 plates at 37° in a humidified air/carbon dioxide (95/5%) atmosphere. Cells were seeded into 48-well plates at a density of 80,000 cells/well in 0.5 mL medium. After 24 hr, plates were treated with 1 μL/well of the following PAHs: 2×10^{-5} M FL, 2×10^{-8} M BkF, 2×10^{-5} M FL + 2×10^{-8} M BkF, 2×10^{-6} M FL + 2×10^{-8} M BkF, 2×10^{-7} M FL + 2×10^{-8} M BkF, 2×10^{-8} M FL + 2×10^{-8} M BkF, and DMSO. Cells were also cotreated with 2×10^{-8} M TCDD + FL. Treatments were run in triplicate on a plate. EROD activity and protein concentrations were determined as described [37], using a CytoFluor 2350 plate reader. Plates were read at 530/590 nm for resorufin production and 400/460 nm for fluorescamine protein determination.

In Vitro *Inhibition of TCDD-Induced Rat Microsomal EROD Activity*

Inhibition of EROD activity was carried out using liver microsomes isolated from female Sprague–Dawley rats treated with TCDD (5 μg/kg). FL (2 μL) was added to the microsomal mixture and incubated for 5 min before the addition of 5 μM ethoxyresorufin. The reaction mixture in each well consisted of 0.1 M HEPES (pH 8.0), 0.01 mg NADPH, 0.01 mg NADH, 0.13 mg BSA, 0.06 mg $MgSO_4$, and 5 μL of microsomes (25 μg microsomal protein). Reactions were carried out for 2 min at 37° in the presence or absence of NADPH. Experimental treatment groups were: DMSO, 2×10^{-4}, 2×10^{-5}, and 2×10^{-7} M FL. EROD activity was determined in triplicate, and results are reported as means with standard deviations. Kinetic studies compared the inhibitory effect of DMSO with that of 2×10^{-4} M FL. Microsomes were incubated for 2 min with DMSO and 0.1, 0.4, and 1.0 μM ethoxyresorufin; for the inhibitory studies, microsomes were incubated for 2 min with FL and 0.1, 0.4, 1.0, 2.5, and 5.0 μM ethyoxyresorufin. The reactions were stopped by the addition of 100 μL methanol.

FL and CYP1A1 mRNA and CYP1A1 Immunoreactive Protein Interactions

Cells were seeded into twenty-one 100 × 20 mm plates in 10 mL α-MEM at a density of approximately 4×10^6 cells/plate. After 24 hr, cells were treated with the following PAHs: 2×10^{-5} M FL, 2×10^{-8} M BkF, 2×10^{-5} M FL + 2×10^{-8} M BkF, 2×10^{-6} M FL + 2×10^{-8} M BkF, 2×10^{-7} M FL + 2×10^{-8} M BkF, 2×10^{-8} M FL + 2×10^{-8} M BkF, and DMSO. Cells were harvested after an additional 24 hr, and mRNA (one plate/treatment) and microsomes (two plates/treatment) were isolated as follows.

Total RNA from cells was extracted using RNA STAT-60 (Tel-Test "B", Inc.). The dried pellet was resuspended in 35 μL formamide by heating at 55°. The RNA was quantitated by UV_{260} absorption. A sample containing 20 μg RNA in 2x sample loading buffer (35% formaldehyde, 10% 10× SPC, 25% TE and 30% 6× tracking dye; the TE solution was 10 mM Tris and 1 mM EDTA, pH 8, and the dye was 0.25% xylene cyanol, 0.25% bromophenol blue, 25% Ficoll, and 0.1 M EDTA) was loaded onto a 1.2% agarose gel (0.66 M formaldehyde) and run at 75 V for 4 hr in 1× SPC buffer (10× SPC contained 200 mM Na_2HPO_4 and 20 mM EDTA, pH 6.8). The gel was stained with ethidium bromide, washed, and transferred to a Hy-

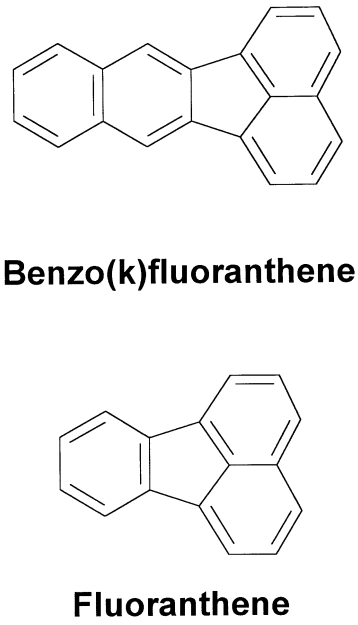

FIG. 1. Structures of benzo(k)fluoranthene (BkF) and fluoranthene (FL).

bond™-N + nucleic acid transfer membrane for a minimum of 12 hr. The membrane was washed in 0.1× SPC, cross-linked by UV exposure, and baked for 2 hr at 80°. The membrane was prehybridized in Denhardt's (1× SSPE, 1% SDS, 10% dextran sulfate, and 0.1% of each polyvinylpyrolidone, bovine serum albumin, and Ficoll; 20× SSPE

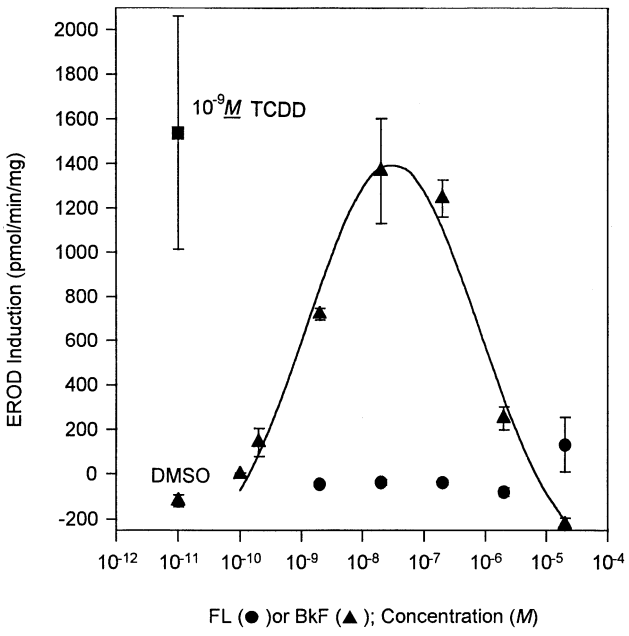

FIG. 2. Representative EROD induction curves for BkF (▲) and FL (●) alone in H4IIE rat hepatoma cells seeded in 48-well plates. Data points represent the mean ± SD of three replicates on a single plate. EROD activities and protein determination were done on a Cytofluor 2350 fluorescent plate reader as described in Materials and Methods. DMSO and TCDD were used as negative and positive controls, respectively.

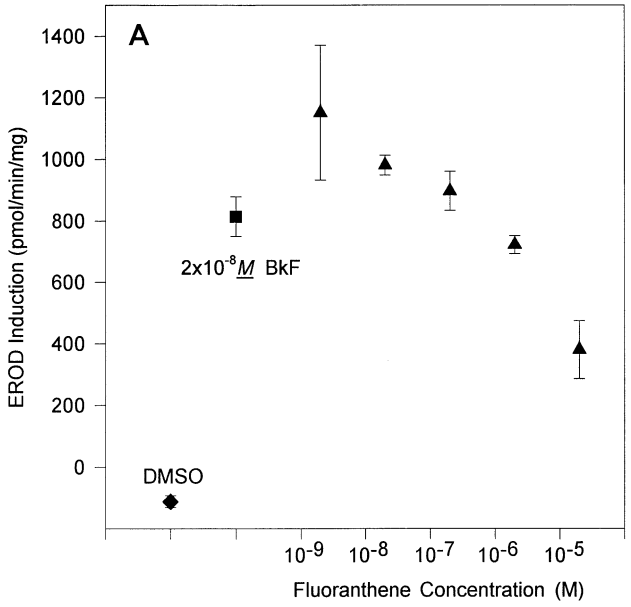

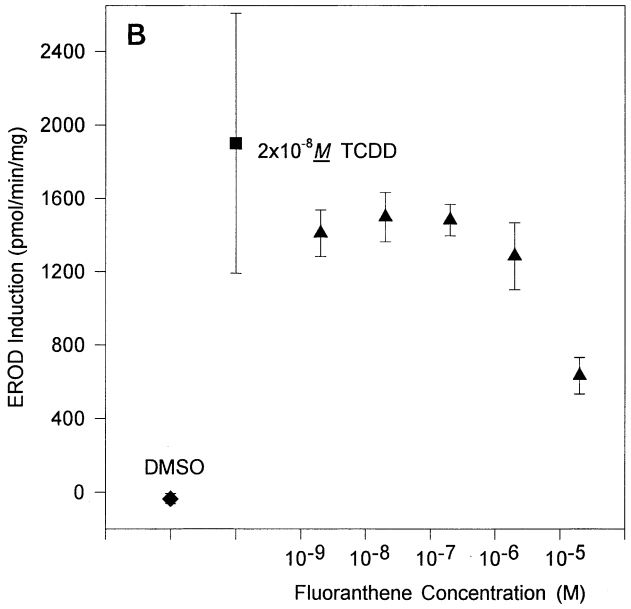

FIG. 3. Induction of EROD activity by BkF alone and in combination with increasing concentrations of FL in H4IIE cells (A). Induction of EROD activity by TCDD alone and in combination with increasing concentrations of FL (B). Data points represent the mean ± SD of three replicates on a single plate. Cotreatment of 2×10^{-5} M FL plus 2×10^{-8} M BkF or TCDD caused significant inhibition of EROD activity ($P = 0.05$). EROD activities were determined using the 48-well plate method as described in Materials and Methods.

contained 3.0 M NaCl, 0.2 M $NaPO_4$, and 0.02 Na_2EDTA) for 12 hr at 65°. Membranes were hybridized for approximately 24 hr in the prehybridizing solution with the addition of 10^6 cpm/mL ^{32}P-randomly labeled probe for P4501A1. CYP1A1 mRNA levels were standardized against β-tubulin mRNA. After hybridization, membranes were washed twice at 20° in 1x SSPE for 15 min. Two additional washes were carried out at 65° for 45 min, each in 1x SSPE and 2% SDS. After a final rinse in distilled

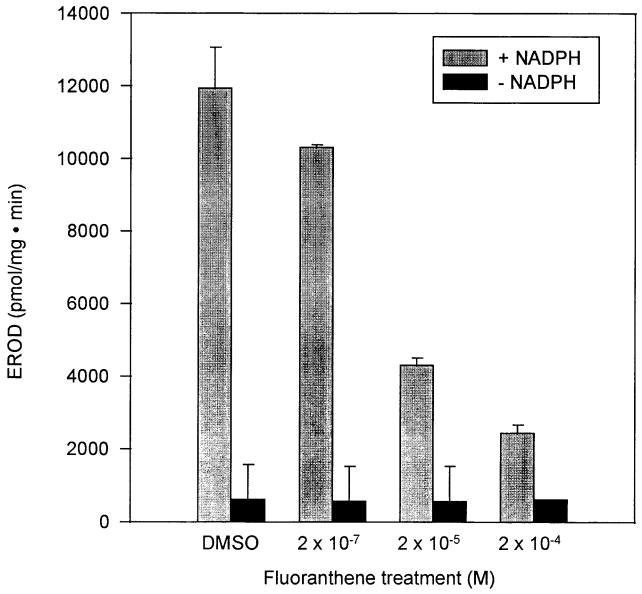

FIG. 4. Inhibition of TCDD-induced EROD activity in rat liver microsomes in the presence of FL. EROD activity was determined using the 96-well microsomal enzyme assay discussed in Materials and Methods. Microsomes were incubated with FL in the presence or absence of NADPH for 5 min prior to the addition of ethoxyresorufin and then incubated for 2 min. Results are presented as the means ± SD for three separate determinations.

water, the membranes were quantitated on a Betagen Betascope 603 blot analyzer imaging system. Finally, the membranes were exposed to X-Omat imaging film (Kodak) and photographed. Membranes were stripped by washing twice in stripping buffer (0.1× SSPE and 1% SDS) at 100°. Each sample was run in triplicate on a northern blot, and means with standard deviations are reported.

Microsomes were prepared by homogenizing cells in buffer (0.25 M sucrose, 0.1 M Tris, pH 7.4). The homogenates were centrifuged at 10,000 *g* for 20 min (4°), and the resulting supernatant was centrifuged at 105,000 *g* for 1 hr at 4°. The microsomal pellet was resuspended in buffer, and proteins were determined by the method of Bradford [38]. Twenty micrograms of microsomal protein was loaded on a 12% minigel as specified for western blot analysis using the rat cytochrome P4501A1 ECL kit (Amersham). Blotting was carried out with the rat P4501A1 antibody as specified by the manufacturer. Results from three western blots are averaged and reported as a percent of BkF positive control ± SD.

DNA Isolation and Adduct Analysis

Cells from two 150 × 25 mm plates were used per replicate, and three replicates per treatment were dosed as follows: DMSO control, BkF 10^{-8} M, BaP 10^{-5} M, FL 10^{-5} M, cotreatment of BkF + FL, and BaP + FL at the same concentrations. DNA was isolated from homogenized cells with RNase A, proteinase K, and extraction with phenol/chloroform/isoamyl alcohol (25:24:1). DNA was precipitated from the aqueous phase with cold ethanol and stored at −20°.

^{32}P-Postlabeling was performed as described previously [39, 40]. Briefly, DNA (12 μg) was digested for 3.5 hr at 37° with 550 mU micrococcal nuclease (Sigma) and 5.5 μg spleen phosphodiesterase (Boehringer Mannheim) in a total volume of 12 μL containing 10 mM calcium chloride and 30 mM sodium succinate, pH 6. Two micrograms of DNA was removed at this point for analysis of normal nucleotides. Then samples were digested further with 9.0 μg Nuclease P1 (Boehringer Mannheim) in a total volume of 15 μL, containing 0.11 mM $ZnCl_2$ and 60 mM sodium acetate, pH 5, for 40 min at 37°. Following the addition of 3 μL of 500 mM 2-(*N*-cyclohexylamino)ethanesulfonic acid (CHES), pH 9.5, the DNA digest was labeled with [γ-^{32}P]ATP (160 μCi; 3000 Ci/mmol) using 12 units of T4 polynucleotide kinase. After incubation for 40 min at 37°, the reaction was terminated with 60 mU potato apyrase (Sigma) over a 30-min period at 37°. Purification and resolution of ^{32}P-labeled adducts were carried out on PEI-cellulose TLC sheets, as described [39, 40] using the following solvents: D1, 2.3 M sodium phosphate, pH 5.7; D3, 3.8 M lithium formate, 6.8 M urea, pH 3.3; D4, 0.72 M sodium phosphate, 0.45 M Tris, 7.7 M urea, pH 8.2. D3 was run to 15 cm from the origin, and D4 was run to 3 cm on a Whatman 1 wick attached to the top of the sheet. RAL values were calculated from the amounts of radioactivity measured, the amount of DNA, and the specific activity of the [^{32}P]ATP used for labeling [39, 40]. Samples were analyzed in triplicate, and RALs are reported with means and standard deviations.

RESULTS

Figure 1 shows the structures of FL and BkF used in this study. The 48-well plate method was used to investigate interactions of both BkF and TCDD, potent EROD inducers, with FL, a relatively poor inducer. Representative induction curves of BkF alone and FL alone are shown in Fig. 2. FL induced minimal EROD activity even at the highest concentration, whereas the EC_{50} for BkF was 4×10^{-10} M. In cells that were cotreated with 2×10^{-8} M BkF or TCDD in the presence of increasing concentrations of FL (up to 2×10^{-5} M), FL decreased both BkF- and TCDD-induced EROD activity (Fig. 3, A and B). Inhibition of EROD activity was investigated further, using liver microsomes from rats treated with TCDD (5 μg/kg). Figure 4 shows that microsomal EROD activity was decreased 14, 64, and 80% after treating microsomes with 2×10^{-7} M, 2×10^{-5} M, and 2×10^{-4} M FL, respectively. The mechanism of the inhibitory response by FL was investigated further in H4IIE cells. Total mRNA was isolated from cells treated with 2×10^{-5} M FL, 2×10^{-8} M BkF, 2×10^{-5} M FL + 2×10^{-8} M BkF, 2×10^{-6} M FL + 2×10^{-8} M BkF, 2×10^{-7} M FL + 2×10^{-8} M BkF, 2×10^{-8} M FL + 2×10^{-8} M BkF, and DMSO. Northern blot results indicated that CYP1A1 mRNA levels were not

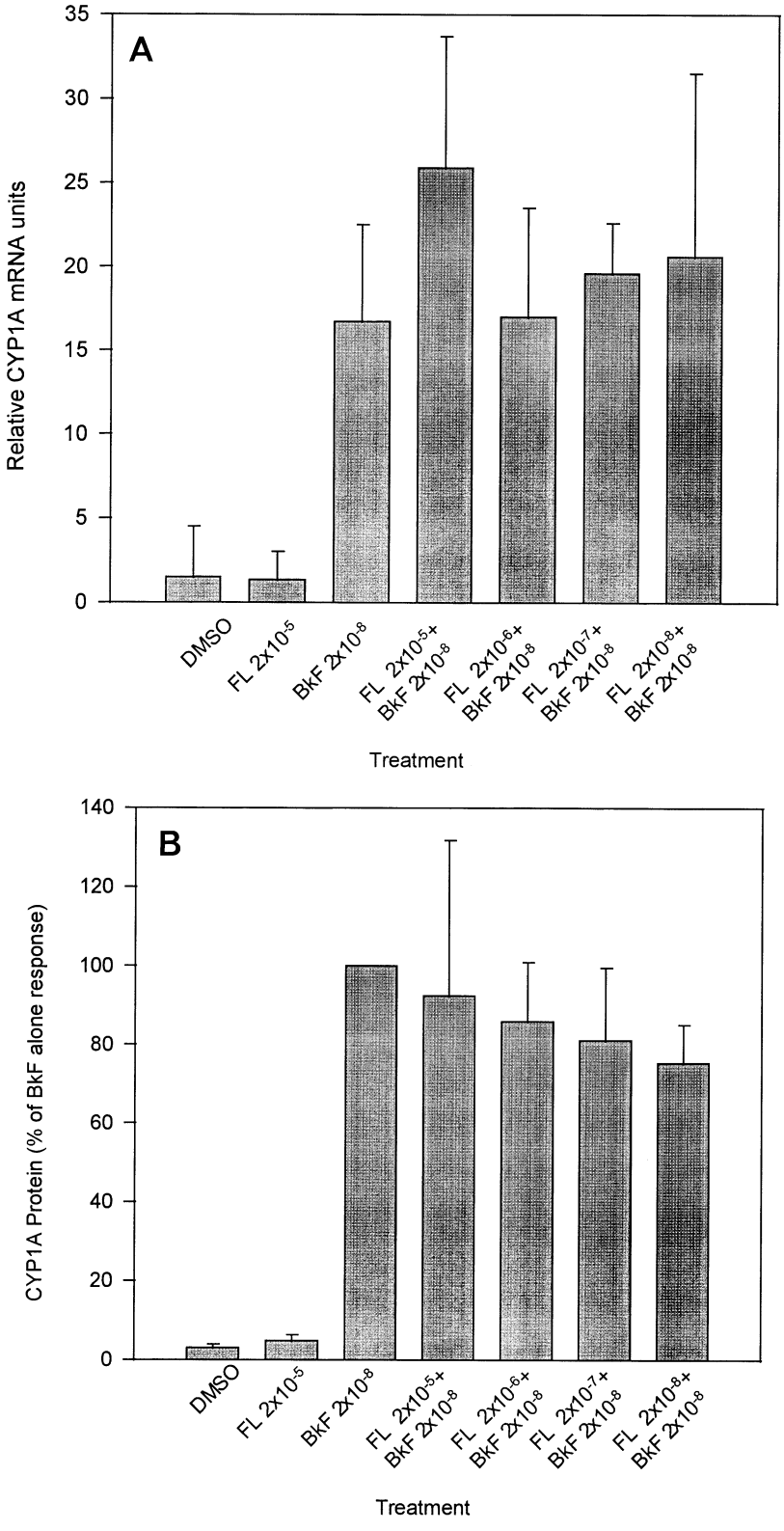

FIG. 5. Relative CYP1A1 mRNA (A) and immunoreactive CYP1A1 protein (B) in H4IIE cells after treatment with DMSO, FL alone, BkF alone, and BkF cotreated with increasing concentrations of FL. Total RNA isolation, northern blot analysis, microsomal preparation, and western blot analysis were done as described in Materials and Methods. CYP1A1 mRNA levels were standardized against β-tubulin mRNA (A). CYP1A1 protein is expressed as the percent of the maximal response observed with BkF alone (100%) (B). Bars represent the mean ± SD of triplicate analysis. There was no significant antagonism of the BkF response in the presence of any concentration of FL (P = 0.05).

decreased significantly in cells cotreated with BkF plus FL compared with levels observed after treatment with BkF alone (Fig. 5A). CYP1A1 mRNA levels in cells treated with FL alone or DMSO (solvent control) were comparable. Likewise, cotreatment with FL did not decrease immunoreactive CYP1A1 protein significantly as determined by western blot analysis (Fig. 5B). Because CYP1A1 mRNA and CYP1A1 immunoreactive protein levels were not decreased in cells cotreated with FL and BkF, the mechanism of inhibition of EROD activity by FL is probably associated with enzyme inhibition or inactivation via covalent modification of CYP1A1. Figure 6 shows the Lin-

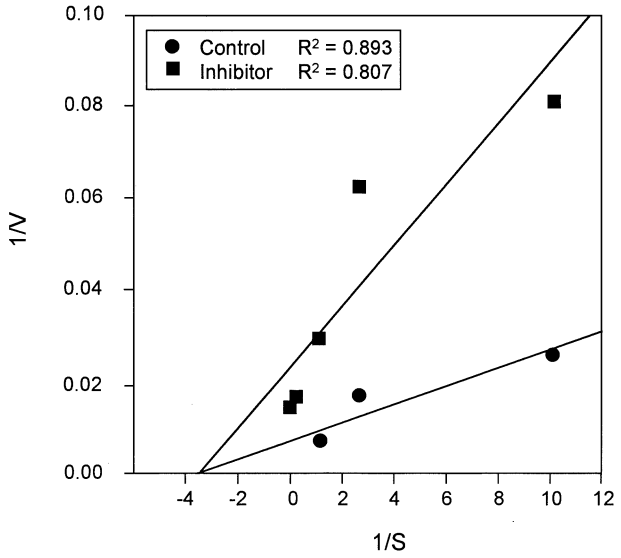

FIG. 6. Lineweaver–Burk plot of FL (2×10^{-5} M) and DMSO indicating noncompetitive inhibition. EROD activity was determined with substrate (ethoxyresorufin) concentrations of 0.1, 0.4, 1.0, 2.5, and 5.0 μM in TCDD-induced rat microsomes as described in Materials and Methods. The K_i for FL inhibition at this concentration was 8.4 μM.

eweaver–Burk plot of data obtained using rat liver microsomal P4501A1 incubated with either DMSO or 2×10^{-5} M FL and 3–5 concentrations of ethoxyresorufin (0.1 to 5 μM). Regression lines through the data points intersected on the X-axis (1/S), indicating noncompetitive inhibition with a K_i of 8.4 μM.

PAH–DNA adduct formation has been correlated with tumor formation in both wildlife and laboratory animals, and therefore the interaction of FL on BaP- or BkF-induced DNA adduct formation was investigated. No consistent adducts were detected by ^{32}P-postlabeling of DNA isolated from FL (10^{-5} M) or DMSO-treated H4IIE cells. The formation of FL–DNA adducts in cells with induced CYP1A1-dependent activity was not determined; however, it is unlikely that these adducts would overlap the higher molecular weight BaP- and BkF-adducts. BaP treatment (10^{-5} M) resulted in 11 adduct spots on the TLC plates, as shown in Fig. 7A. Cotreatment of BaP and FL increased the relative adduct labeling per 10^9 normal nucleotides (RAL) of spots 2, 4, and 6 approximately 2-fold (Fig. 7B, Table 1) from 622 to 1158 ($P = 0.03$). Spot 8, while a major adduct, remained unchanged in cells treated with BaP plus FL. Spot 4 was the main adduct when H4IIE cells were treated with 10^{-8} M BkF (Fig. 7C). A significant increase in RAL of this adduct was observed in cells cotreated with BkF plus FL (3.6 vs 8.8) as shown in Fig. 7D and Table 1.

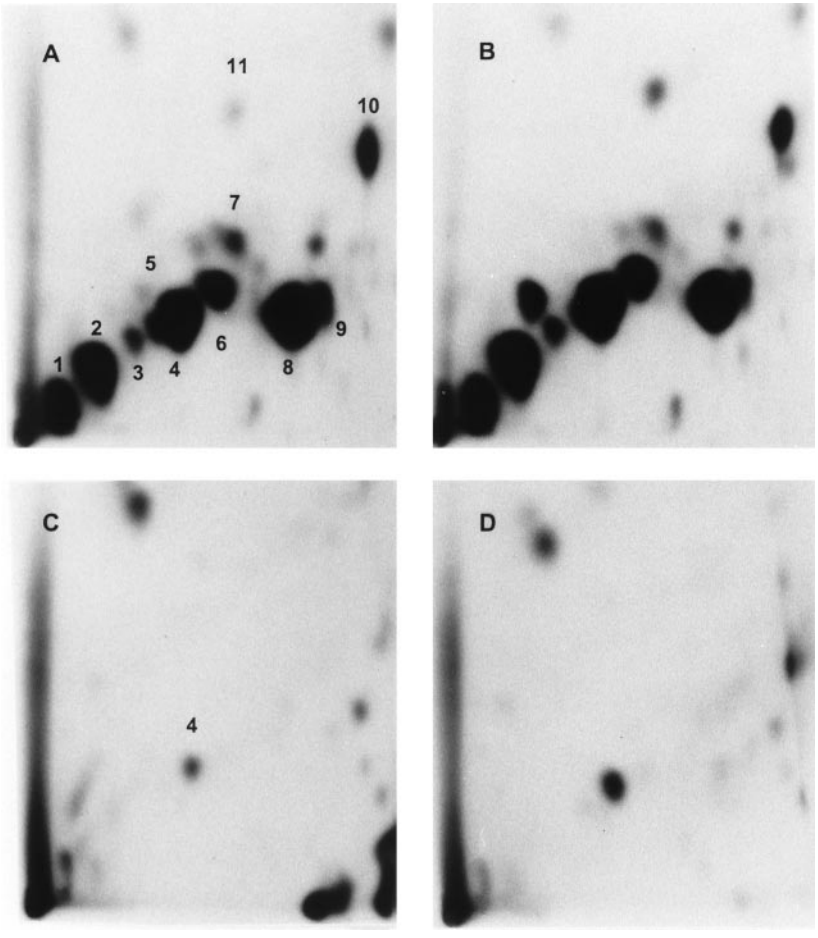

FIG. 7. Thin-layer chromatography plates showing ^{32}P-postlabeled PAH–DNA adducts in H4IIE cells. (A) Eleven adduct spots and an internal standard resulted when cells were treated with 10^{-5} M BaP. (B) Spots 2, 4, and 6 were increased approximately 2-fold when cells were cotreated with 10^{-5} M BaP and 10^{-5} M FL. (C) Spot 4 was the major spot with 10^{-8} M BkF treatment. (D) Spot 4 was increased approximately 2-fold when cells were cotreated with 10^{-5} M FL and 10^{-8} M BkF. The ^{32}P-postlabeling procedure is described in Materials and Methods ($N = 3$, P values indicated in Table 1).

TABLE 1. DNA adduct results for H4IIE cells treated with BaP or BkF alone or in combination with FL*

Spots	RAL values BaP	BaP + FL	*P*
1	197 ± 8	192 ± 12	0.56
2	268 ± 25	487 ± 93†	0.02
3	10 ± 1	16 ± 4	0.07
4	287 ± 12	535 ± 151†	0.05
5	22 ± 14	51 ± 14	0.07
6	67 ± 2	136 ± 32†	0.02
7	12 ± 1	14 ± 3	0.38
8	878 ± 77	768 ± 162	0.35
9	24 ± 4	18 ± 2†	0.05
10	55 ± 14	49 ± 8	0.6
11	6 ± 2	11 ± 4	0.13
Sum 2,4,6	622 ± 23	1158 ± 276†	0.03
	BkF	BkF + FL	
4	3.6 ± 0.8	8.8 ± 0.5†	< 0.001

* Treatment of H4IIE cells and ^{32}P-postlabeling experiments were conducted in triplicate as described in Materials and Methods. RAL values (mean ± SD) for each spot per 10^9 normal nucleotides are reported.

† Cotreatment with FL significantly increased adduct intensity ($P < 0.05$).

While FL inhibited CYP1A-mediated EROD activities, it enhanced some PAH–DNA adducts.

DISCUSSION

FL is detected frequently in PAH-contaminated extracts and areas [2, 22–24]. FL has been identified in urban soil at concentrations between 200 and 166,000 μg/kg, where BaP concentrations were only 165 to 220 μg/kg [1]. Likewise, mussels collected from Dorchester Bay, MA, had approximately 450 and 25 ng/g dry weight of FL and BkF, respectively, in their tissues [23]. Therefore, the concentration of FL may be significantly higher than the carcinogenic PAHs in some environmental samples. For this reason, interactions of PAHs in the H4IIE bioassay were investigated using BkF and TCDD, both potent inducers of EROD activity, in the presence of increasing concentrations of FL and several other lower molecular weight PAHs that are also found in the environment. As shown in Fig. 3, both TCDD and BkF alone induced EROD activity, and this was decreased significantly in the presence of 2×10^{-5} M FL. This inhibitory response was not observed for fluorene, phenanthrene, or acenaphthene. Likewise, when rat liver microsomal P4501A1 from TCDD-treated rats was incubated with FL, EROD activity was also inhibited up to 80% with 2×10^{-4} M FL (Fig. 4).

The mechanism of inhibition of CYP1A1 by FL was investigated further by quantitating CYP1A1 mRNA and CYP1A1 immunoreactive protein levels. The results showed that there was not a significant decrease of mRNA or immunoreactive protein levels in H4IIE cells cotreated with FL plus BkF (Fig. 5, A and B). Because CYP1A1 was not inhibited by FL at either the message or protein level, the mechanism of inhibition appears to be associated with inhibition of enzyme activity. Lineweaver–Burk analysis of microsomal P4501A1 treated with DMSO or 2×10^{-5} FL and increasing concentrations of ethoxyresorufin indicated noncompetitive inhibition by FL with a K_i of 8.4 μM. Direct inhibition of enzyme activity (EROD) has been reported previously in PLHC-1 fish hepatoma cells cotreated with 3-methylcholanthrene (3-MC) and tributyltin (TBT) [25]. Organotins caused a 50% inhibition of EROD activity in induced PLHC-1 lysates at 4.7×10^{-5} and 6.7×10^{-5} M for TBT and dibutyltin, respectively. Aminoanthracene (AA) has been reported to cause a 66.5% decrease in EROD activity in β-naphthoflavone-induced channel catfish [26]. Time-dependent inhibition of EROD activity by AA was observed in hepatic microsomes following both *in vivo* and *in vitro* exposures. These studies concluded that AA is a mechanism-based inactivator (suicide substrate) of CYP1A in hepatic tissue of channel catfish. The current study shows that FL is also a noncompetitive inhibitor of CYP1A1-dependent activity. These results are the first to show that an environmentally relevant PAH is an inhibitor of CYP1A1-mediated activity.

The implications of this inhibitory response by FL are important for development of an induction equivalency approach for assessment of PAH-containing samples [13, 41, 42]. The H4IIE bioassay assumes additivity of the inducing compounds by the following equation: $EQ_{extract} = \Sigma([PAH]_1EF_1 + \ldots + [PAH]_nEF_n)$. Previous research in our laboratory has indicated that when EFs for seven inducing PAHs were determined, the EQ approach was effective in predicting bioassay results in PAH-treated oyster samples [13]. However, because FL inhibits EROD activity, bioassay EQs will underestimate the true potency of extracts containing relatively high levels of FL. For example, some urban soil samples have an FL to BaP ratio of about 750 [1], and this ratio could be even higher in other matrices or species from contaminated areas.

The potential effects of FL on the genotoxicity of PAHs were also investigated in H4IIE cells cotreated with FL plus two carcinogenic PAHs, BaP or BkF. PAH–DNA adduct analysis indicated that both BaP and BkF DNA adducts were increased in H4IIE cells after cotreatment with FL. Spot 4 in Fig. 7A and B chromatographs with the (+)-anti-BaP-7,8-diol-9,10 epoxide adduct at the N-2 position of deoxyguanosine [40], and formation of this adduct has been correlated with tumor formation in various animals [35, 36, 43]. This adduct was increased from 287 to 535 RAL × 10^9 in cells cotreated with BaP plus FL. CYP1A1 can enhance or inhibit metabolic activation of PAHs, and the results of this study show that inhibition of CYP1A1-dependent activity by FL resulted in increased adduct levels. FL may also affect other enzyme activities associated with PAH metabolism; however, these activities have not been investigated in this study. This result highlights another drawback of the induction equivalency-based bioassay for PAH mixtures. The EQ system assumes that all of the compounds act additively and through the same mechanism of action. It is clear from these studies that while FL

inhibits induced EROD activity in the H4IIE bioassay (Fig. 3 and 4), this same compound increases the potential genotoxicity of BaP and BkF by enhancing formation of some PAH–DNA adducts (Table 1). Current research is focused on the limitations of the induction equivalency based bioassays for PAHs and the interactions of FL with carcinogenic PAHs and the effects on their genotoxicity in both cellular and *in vivo* models.

The financial assistance of the National Institutes of Health (ES-04917) and the Electric Power Research Institute is gratefully acknowledged. We also thank Natalie Pong for supplying technical assistance.

References

1. ATSDR, *Toxicological Profile for Polycyclic Aromatic Hydrocarbons (PAHs)*. ATSDR, Atlanta, GA, 1995.
2. Freeman DJ and Cattell FC, Woodburning as a source of atmospheric polycyclic aromatic hydrocarbons. *Environ Sci Technol* **24:** 1581–1585, 1990.
3. Witt G, Polycyclic aromatic hydrocarbons in water and sediment of the Baltic Sea. *Mar Pollut Bull* **31:** 237–248, 1995.
4. Fabacher DL, Schmitt CJ, Besser JM and Mac MJ, Chemical characterization and mutagenic properties of polycyclic aromatic compounds in sediment from tributaries of the Great Lakes. *Environ Toxicol Chem* **7:** 529–543, 1988.
5. Broman D, Naf C, Rolff C and Zebuhr Y, Occurrence and dynamics of polychlorinated dibenzo-*p*-dioxins and dibenzofurans and polycyclic aromatic hydrocarbons in a mixed surface layer of remote coastal and offshore waters of the Baltic. *Environ Sci Technol* **25:** 1850–1863, 1991.
6. Shaw GR and Connell DW, Prediction and monitoring of the carcinogenicity of polycyclic aromatic compounds (PACs). *Rev Environ Contam Toxicol* **135:** 1–62, 1994.
7. Mastrangelo G, Fadda E and Marzia V, Polycyclic aromatic hydrocarbons and cancer in man. *Environ Health Perspect* **104:** 1166–1170, 1996.
8. Vogelbein WK, Fournie JW, Van Veld PA and Huggett RJ, Hepatic neoplasms in the mummichog *Fundulus heteroclitus* from a creosote-contaminated site. *Cancer Res* **50:** 5978–5986, 1990.
9. Yamaguchi K, Near R, Shneider A, Cui H, Ju S-T and Sherr DH, Fluoranthene-induced apoptosis in murine T cell hybridomas is independent of the aromatic hydrocarbon receptor. *Toxicol Appl Pharmacol* **139:** 144–152, 1996.
10. Rice JE, Hosted TJ Jr and Lavoie EJ, Fluoranthene and pyrene enhance benzo[*a*]pyrene–DNA adduct formation *in vivo* in mouse skin. *Cancer Lett* **24:** 327–333, 1984.
11. Wang J-S and Busby WF, Induction of lung and liver tumors by fluoranthene in a preweaning CD-1 mouse assay. *Carcinogenesis* **14:** 1871–1874, 1993.
12. Wang J-S, Busby WF Jr and Wogan GN, Formation and persistence of DNA adducts in organs of CD-1 mice treated with a tumorigenic dose of fluoranthene. *Carcinogenesis* **16:** 2609–2616, 1995.
13. Willett KL, Gardinali PR, Sericano JL, Wade TL and Safe SH, Characterization of the rat hepatoma cell bioassay for evaluation of environmental samples containing polynuclear aromatic hydrocarbons (PAHs). *Arch Environ Contam Toxicol* **32:** 442–448, 1997.
14. Anderson J, Bothner K, Edelman D and Vincent S, P450 TGS: A biomarker for assessing the toxicity of environmental samples. *TAPPI Int Environ Conference* **1:** 21–28, 1995.
15. Zacharewski T, Safe L, Safe S, Chittim B, DeVault D, Wiberg K, Bergqvist P and Rappe C, Comparative analysis of polychlorinated dibenzo-*p*-dioxin and dibenzofuran congeners in Great Lakes fish extracts by gas chromatography–mass spectrometry and *in vitro* enzyme induction activities. *Environ Sci Technol* **23:** 730–735, 1989.
16. Tysklind M, Tillitt D, Ericksson L, Lundgren K and Rappe C, A toxic equivalency factor scale for polychlorinated dibenzofurans. *Fundam Appl Toxicol* **22:** 277–285, 1994.
17. Tillitt DE, Giesy JP and Ankley GT, Characterization of the H4IIE rat hepatoma cell bioassay as a tool for assessing toxic potency of planar halogenated hydrocarbons in environmental samples. *Environ Sci Technol* **25:** 87–92, 1991.
18. Schmitz H-J, Hagenmaier A, Hagenmaier H-P, Bock KW and Schrenk D, Potency of mixtures of polychlorinated biphenyls as inducers of dioxin receptor-regulated CYP1A activity in rat hepatocytes and H4IIE cells. *Toxicology* **99:** 47–54, 1995.
19. Piskorska-Pliszczynska J, Keys B, Safe S and Newman MS, The cytosolic receptor binding affinities and AHH induction potencies of 29 polynuclear aromatic hydrocarbons. *Toxicol Lett* **34:** 67–74, 1986.
20. Willett K, Gardinali P and Safe S, Induction equivalency factors for halogenated aromatic hydrocarbons and polynuclear aromatic hydrocarbons using the H4IIE rat hepatoma bioassay. *Organohalogen Cmpds* **29:** 375–379, 1996.
21. Hahn ME, Lamb TM, Schultz ME, Smolowitz RM and Stegeman JJ, Cytochrome P4501A induction and inhibition by 3,3′,4,4′-tetrachlorobiphenyl in an Ah receptor-containing fish hepatoma cell line (PLHC-1). *Aquat Toxicol (Amsterdam)* **26:** 185–208, 1993.
22. Diamond SA, Oris JT and Guttman SI, Adaptation to fluoranthene exposure in a laboratory population of fathead minnows. *Environ Toxicol Chem* **14:** 1393–1400, 1995.
23. Peven CS, Uhler AD and Querzoli FJ, Caged mussels and semipermeable membrane devices as indicators of organic contaminant uptake in Dorchester and Duxbury Bays, Massachusetts. *Environ Toxicol Chem* **15:** 144–149, 1996.
24. Ruokojarvi P, Ruuskanen J, Ettala M, Rahkonen P and Tarhanen J, Formation of polyaromatic hydrocarbons and polychlorinated organic compounds in municipal waste landfill fires. *Chemosphere* **31:** 3899–3908, 1995.
25. Bruschweiler BJ, Wurgler FE and Fent K, Inhibition of cytochrome P4501A by organotins in fish hepatoma cells PLHC-1. *Environ Toxicol Chem* **15:** 728–735, 1996.
26. Watson DE, Ménard L, Stegeman JJ and Di Giulio RT, Aminoanthracene is a mechanism-based inactivator of CYP1A in channel catfish hepatic tissue. *Toxicol Appl Pharmacol* **135:** 208–215, 1995.
27. Lu Y-F, Santostefano M, Cunningham BDM, Threadgill MD and Safe S, Identification of 3′-methoxy-4′-nitroflavone as a pure aryl hydrocarbon (Ah) receptor antagonist and evidence for more than one form of the nuclear Ah receptor in MCF-7 human breast cancer cells. *Arch Biochem Biophys* **316:** 470–477, 1995.
28. Liu H, Santostefano M and Safe S, 2-Phenylphenanthridinone and related compounds: Aryl hydrocarbon receptor agonists and suicide inactivators of P4501A1. *Arch Biochem Biophys* **313:** 206–214, 1994.
29. Kao LR and Wilkinson CF, Inhibition of cytochrome P-450c-mediated benzo[*a*]pyrene hydroxylase and ethoxyresorufin O-deethylase by dihydrosafrole. *Xenobiotica* **17:** 793–805, 1987.
30. Merchant M and Safe S, *In vitro* inhibition of 2,3,7,8-tetrachlorodibenzo-*p*-dioxin-induced activity by α-naphthoflavone and 6-methyl-1,3,8-trichlorodibenzofuran using an aryl hydrocarbon (Ah)-responsive construct. *Biochem Pharmacol* **50:** 663–668, 1995.
31. Grafstom R and Stohs SJ, Inhibitors of 7-ethoxyresorufin and 7-ethoxycoumarin de-ethylases in rat small intestinal microsomes and cells. *Drug Chem Toxicol* **4:** 147–159, 1981.

32. Chang TKH, Gonzalez FJ and Waxman DJ, Evaluation of triacetyloleandomycin, α-naphthoflavone, and diethyldithiocarbamate as selective chemical probes for inhibition of human cytochromes P-450. *Arch Biochem Biophys* **311:** 437–442, 1994.
33. Randerath K and Randerath E, ^{32}P-Postlabeling methods for DNA adduct detection: Overview and critical evaluation. *Drug Metab Rev* **26:** 67–85, 1994.
34. Weyland EH, Cai Z, Wu Y, Rice JE, He Z and Lavoie EJ, Detection of the major DNA adducts of benzo[b]fluoranthene: Role of phenolic dihydrodiols. *Chem Res Toxicol* **6:** 568–577, 1993.
35. Hall M and Grover PL, Polycyclic aromatic hydrocarbons, metabolism, activation, and tumor initiation. In: *Chemical Carcinogenesis and Mutagenesis I* (Eds. Cooper CS and Grover PL), pp. 327–372. Springer, London, 1990.
36. Varanasi U, Reichert WL, Eberhart BL and Stein JE, Formation and persistence of benzo(a)pyrene-diol epoxide–DNA adducts in liver of English sole (*Parophrys vetulus*). *Chem Biol Interact* **69:** 203–216, 1989.
37. Kennedy SW and Jones SP, Simultaneous measurement of cytochrome P4501A catalytic activity and total protein concentration with a fluorescence plate reader. *Anal Biochem* **222:** 217–223, 1994.
38. Bradford MM, A rapid and sensitive method for the quantitation of microgram quantities of protein utilizing the principle of protein-dye binding. *Anal Biochem* **72:** 248–254, 1976.
39. Reddy MV and Randerath K, Nuclease P1-mediated enhancement of sensitivity of ^{32}P-postlabeling test for structurally diverse DNA adducts. *Carcinogenesis* **7:** 1543–1551, 1986.
40. Randerath E, Zhou G-D, Donnelly KC, Safe SH and Randerath K, DNA damage induced in mouse tissues by organic wood preserving waste extracts as assayed by ^{32}P-postlabeling. *Arch Toxicol* **70:** 683–695, 1996.
41. Chaloupka K, Harper N, Krishnan V, Santostefano M, Rodriguez LV and Safe S, Synergistic activity of aromatic hydrocarbon mixtures as aryl hydrocarbon (Ah) receptor agonists. *Chem Biol Interact* **89:** 141–158, 1993.
42. Chaloupka K, Steinberg M, Santostefano M, Rodriguez LV, Goldstein L and Safe S, Induction of *Cyp1a-1* and *Cyp1a-2* gene expression by a reconstituted mixture of polynuclear aromatic hydrocarbons in B6C3F1 mice. *Chem Biol Interact* **96:** 207–221, 1995.
43. Smolarek TA, Morgan SL, Moynihan CG, Lee H, Harvey RG and Baird WM, Metabolism and DNA adduct formation of benzo[a]pyrene and 7,12-dimethylbenz[a]anthracene in fish cell lines in culture. *Carcinogenesis* **8:** 1501–1509, 1987.